DOI: 10.1016/S1872-5805(21)60023-16

Preparation of graphene/copper nanocomposites by ball milling followed by pressureless vacuum sintering

HU Zeng-rong[1,2], DAI Rui[3], WANG Di-ni[3], WANG Xiao-nan[2,4], CHEN Feng[5], FAN Xue-liang[1], CHEN Chang-jun[6], LIAO Yi-liang[7], NIAN Qiong[3,*]

(1. *School of Rail Transportation*, *Soochow University*, *Suzhou* 215131, *China*;
2. *High-performance Metal Structural Materials Research Institute*, *Soochow University*, *Suzhou* 215131, *China*;
3. *Department of Mechanical Engineering*, *Arizona State University*, *Tempe*, *AZ* 85281, *USA*;
4. *Shagang School of Iron and Steel*, *Soochow University*, *Suzhou* 215131, *China*;
5. *College of Mechanical and Electrical Engineering*, *Nanjing University of Aeronautics and Astronautics*, *Nanjing* 210016, *China*;
6. *College of Mechanical and Electrical Engineering*, *Soochow University*, *Suzhou* 215131, *China*;
7. *Department of Mechanical Engineering*, *University of Nevada*, *Reno*, *NV* 89557, *USA*)

Abstract: Graphene has been considered as an ideal reinforcement filler for metal matrix composites because of its ultra-high strength and stiffness, and exceptional thermal and electrical properties. Graphene-reinforced copper (Gr/Cu) nanocomposites were fabricated by ball milling followed by pressureless vacuum sintering, and were characterized by SEM, TEM, XRD, Raman spectroscopy and mechanical tests. Results indicate that the graphene platelets are well dispersed in the nanocomposites without apparent damage. The graphene filler dramatically improves the hardness and reduces the coefficient of friction of the Gr/Cu nanocomposites compared to pure Cu.

Key words: Nanocomposite; Graphene; Copper; Pressureless sintering

1 Introduction

Copper-based metal matrix composites (MMCs) have been known for their exceptional physical properties, such as excellent mechanical strength, dimension stability, creep resistance, excellent cyclic fatigue characteristics, and distinctive electrical and thermal properties. These outstanding characteristics broaden applications of copper-based MMCs in the industrial fields like aerospace, automobile, national security, and electronic sectors. Previously, it has been demonstrated the performance of MMCs is mainly determined by the reinforcement fillers in the metal matrices. There are plenty of conventional reinforcement fillers utilized in MMCs, e.g., nitride ceramic (TiN, BN), oxide ceramic (Al_2O_3, SiO_2), and carbides (TiC, WC). However, most of these ceramic reinforcements possess poor thermal or electrical properties. Consequently, these reinforcements improve the mechanical properties, but at a sacrifice of the electrical and thermal properties. In recent years, carbon allotropes including carbon nanotubes (CNTs) and graphene are investigated extensively as ideal reinforcement fillers for MMCs. For instance, Bakshi summarized in his review that enormous research studies had been carried out on CNT-reinforced MMCs in the past decade and had demonstrated the potential benefit of CNTs in MMCs for improvement of mechanical properties[1]. In spite of these efforts, Neubauer pointed out that the practical application of CNTs is limited by its difficult dispersion caused by the high electrostatic and van der Waals forces, as well as its high production cost[2].

At the same time, another carbon allotrope, graphene, has attracted considerable attentions in MMCs field owing to its good dispersion in the metal matrix and cost-effective manufacturing through graphite exfoliation. As Sun reported, the Hummers method was modified with a spontaneous expansion process to prepare graphene, which enabled it to be-

Received date: 2019-07-24; **Revised date:** 2020-01-13

Corresponding author: NIAN Qiong, Professor. E-mail: Qiong.Nian@asu.edu

Author introduction: HU Zeng-rong. E-mail: zengronghu@126.com

Supplementary data associated with this article can be found in the online version.

come facile and practical for scalable production of graphene oxide (GO) and reduced GO[3]. Additionally, graphene reinforced MMCs exhibit impressive improvement in mechanical and physical properties, owing to the exceptional properties of graphene such as high thermal conductivity, electrical conductivity, Young's modulus, and tensile strength, in comparison to the intrinsic metal counterpart. Thereby, a variety of metal matrices have been investigated using graphene as a filler such as Al, Ni, Cu, Mg, Ti and Fe as reviewed by Hu[4]. Except for Bartolucci[5] who claimed a lower strength and hardness of graphene reinforced aluminum which was caused by excessive Al_4C_3 produced during the fabricating process, all other reports in this field reported improvements in mechanical properties of MMCs. Among various metals, copper and copper alloys are indispensable materials in many industrial fields, including electrical, electronic and bearing industry. Li et al. pointed out that the inherent high thermal and electrical conductivity of copper combined with the excellent properties of graphene will lead to the formation of high-performance composites, which can be widely used in many industrial fields[6]. Thus, it is highly desirable to develop graphene reinforced copper matrix nanocomposites from the practical perspective.

In order to fabricate graphene reinforced copper matrix nanocomposites, in this work, a pressureless vacuum sintering process after ball milling has been investigated. Mechanical ball milling is extensively used to produce alloys from powders due to its efficacy in grinding and cold welding. Its effectiveness also has been demonstrated in dispersion graphene flakes in metal powder matrix. Pérez-Bustamante found that when the high energy ball milling technology was used to prepare the mixture of graphene and Al powder, graphene sheets can be dispersed in the aluminum powder in short periods of milling time. Kim also stated that ball milling was effective in preparing a mixture of graphene and copper powder[7, 8]. On the other hand, vacuum sintering is a proven technology and widely used in powder metallurgy, but to the best of our knowledge, there is still no reports that it can be applied in the graphene reinforced MMCs. Although vacuum sintering process is time-consuming comparing with spark plasma sintering (SPS), it provides more flexibility for fabricating complicated geometry. What's more, embedding graphene in copper matrix can prevent its oxidation, therefore lower the damaging possibility in long heating cycle. Thus, this pressureless sintering process was investigated and the tribological behavior of as-fabricated nanocomposites were studied in this work.

2 Experimental

2.1 Materials

The Cu powder (99.5%, average diameter ~ 30 μm, Tianjin Chemical Reagent Co. Ltd, China) and multi-layer graphene platelets (<5 layers, Nanjing Kefu Nanotech Inc., China) as shown in Fig. S1, were used in ball milling and vacuum sintering experiments. The Cu powder and graphene platelets were mixed together by a planetary ball mill (speed 300 r min^{-1}, 2 h, stainless steel ball, ϕ 8 mm, stainless jar). The ratio of ball to powder was 5∶1, and ball milling was carried out in ambient conditions. The powder mixtures had four different weight ratios, namely, Cu, Cu-1 wt. % Gr, Cu-2.5 wt. % Gr, and Cu-5 wt. % Gr, as shown in Fig. 1a-d. No agglomeration of graphene has been observed in these mixtures.

2.2 Sample preparation

Each of the ball milled mixture was compressed into a cubic compact of 20×20×2 mm^3 under a uniaxial pressure of 500 MPa in a die mold. And then all the compressed samples were sintered in a tube vacuum furnace (GSL-1700X-S, Dachun, Hefei, China). In particular, the compressed samples were put into an Al_2O_3 square crucible in one layer, which would be further put into the tube vacuum furnace. The furnace was evacuated to 50 mTorr (the max vacuum degree of the equipment), filled with argon gas to 1 stand atmospheric pressure, then evacuated to 50 mTorr again. This process was repeated three times to ensure minimum oxygen residue remaining in the furnace. The temperature evolution during vacuum sintering process is shown in Fig. 1e, where the inserted image shows the sintered Gr-Cu nanocomposites.

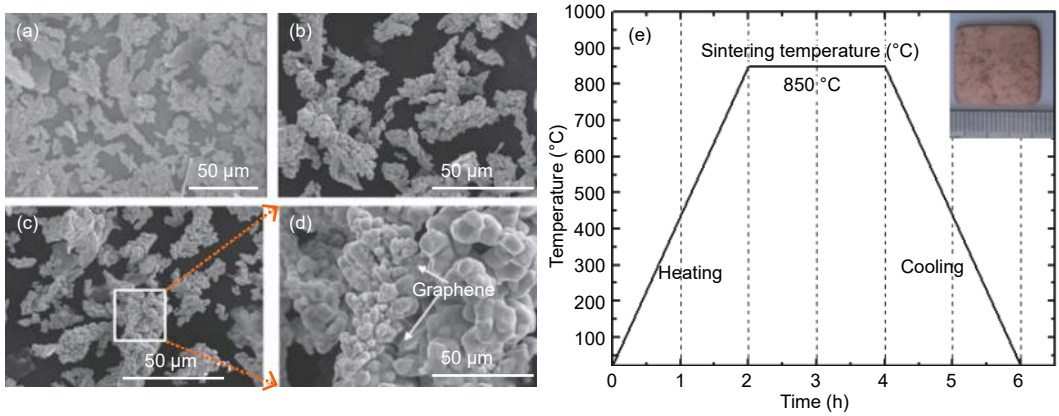

Fig. 1 SEM images of (a) 1 wt. % Gr/Cu mixture, and (b) 2.5 wt. % Gr/Cu mixture, (c) 5 wt %Gr/Cu mixture, (d) focused-in observation of 5 wt. %Gr/Cu mixture and (e) temperature profile of vacuum sintering process, the insert image shows the photo of the sintered nanocomposite sample.

2.3 Microstructure characterization

A Rigaku UltimaⅣ Miltipurpose X-Ray diffraction system was employed to check the samples with Cu-Kα source. Hitachi S-4700 Field emission and Hitachi SU5000 SEM were used to get the microstructural images. The Raman spectra were obtained with A HORIBA LabRAM HR800 Raman spectrometer (HORIBA Jobin Yvon, NJ, USA). TEM samples were prepared by a TenuPol-5 twin-jet electropolishing system via a twin-jet electropolishing method. Microstructure images were recorded by an FEI Tecnai G-20 system at a 200 keV operating voltage.

2.4 Mechanical property testing

The micro-hardness of samples was measured by an HXD- 1000TM/LCD (Shanghai optical instrument factory, Shanghai, China) micro-hardness instrument (100 g load, 10 s holding time). The test surface was polished by a metallographic polishing machine to get a sufficiently good surface before testing.

3 Results and discussion

Fig. 2a-d shows the surface morphology of the vacuum sintered Gr-Cu nanocomposites in three different graphene weight ratios, as well as the bare copper sample. The SEM images reveal that both of the bare Cu and Gr-Cu nanocomposites have a similar surface morphology, with a minimized discontinued pore area. Increasing the graphene ratio, the sample surface becomes more discontinued resulting from filling of graphene sheets in the copper matrix. Chu et al mentioned in his work that graphene flakes can also block the copper powder from merging together, thereby bringing about a grain refinement phenomena[9], which explains the small grains observed in our nanocomposites.

In order to further review the morphology of the nanocomposites, focused-in view through SEM and TEM has been conducted in Fig. 2e-g. The magnified SEM image in Fig. 2e is the sintered 2.5 wt. % Gr-Cu nanocomposite. It can be seen that copper particles are sintered together, and there are obvious curve marks between metal particles. This could be explained by the fact that the sintering temperature selected herein is lower than the melting point of copper. In this respect, the copper phase is lack of sufficient diffusion in solid state sintering reaction. Thus, it cannot form a uniform or dense surface commonly observed in liquid state sintering reaction. Consequently, the low diffusion rate will also affect the bonding status between graphene sheets and copper phase. As pointed out by Xu et al, who studied the structural and mechanical relationship at a graphene-metal interface through density functional theory based on calculations, compared with other metals, copper has a relatively lower bonding energy to graphene[10]. Fig. 2f is the cross-sectional surface morphology of the 5 wt. % Gr-Cu nanocomposite. Graphene sheets can be found embedded inside the copper matrix. In this image, however, porous area inside the composite still can be observed. The insufficiently densified microstructure is prone to weaken the mechanical strength/hardness

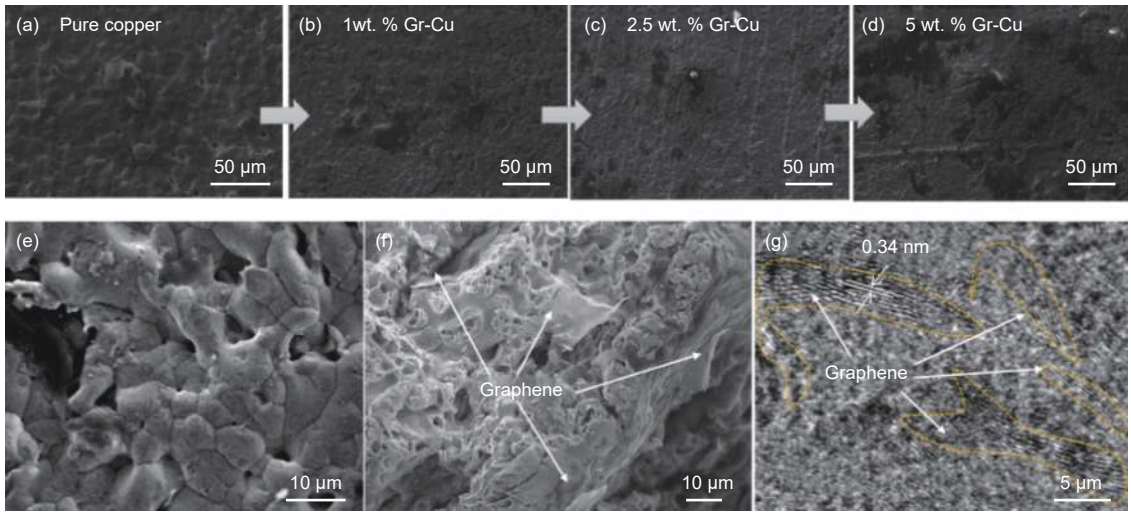

Fig. 2　Surface morphology of vacuum sintered (a) Cu, (b) 1 wt. % Gr/Cu, (c) 2.5 wt. % Gr/Cu, (d) 5 wt. % Gr/Cu nanocomposites, (e) magnified observation of 2.5 wt. % Gr/Cu, (f) sectional morphology of 5 wt. % Gr/Cu and (g) TEM image of 5 wt. % Gr/Cu composites.

of the nanocomposites but on the other hand, it will benefit the tribological performance, especially in the situation of liquid oil lubrication, since the oil can be held in the porous area. The further characterization of this 5 wt. % Gr-Cu composite by TEM image in Fig. 2g shows the direct observation of multilayer graphene sheets embedded in the copper matrix. The areas marked by the yellow dashed line indicate graphene sheets. And the distance between two graphene layers, 0.34 nm can be measured to confirm the graphene phase. The multi-layer characteristic can be determined by the graphene layer number in the image.

In order to confirm the existence of graphene sheets in the sintered nanocomposites, both XRD patterns and Raman spectra were collected. Fig. 3a shows the XRD patterns of vacuum sintered Gr-Cu nanocomposites. Firstly, there are peaks at 2θ degree of about 43°, 50°, 74° and 90°, which are well indexed to (111), (200), (220) and (311) for Cu (PDF #03-1 005: 2004), respectively. There is an extremely weak diffraction peak on Gr-Cu XRD patterns at 2θ degree of about 39.9°, which can be indexed as CuO (200) peak. Correspondingly, the CuO phase is also observed on HRTEM image of Gr-Cu samples, as shown in Fig. S2. The existence of CuO in the vacuum sintered Gr-Cu nanocomposites might result from the fact that the samples are kept in ambient environment after sintering, therefore copper atoms on the surface would inevitably react with oxygen in air. And the graphene platelets are purchased from the commercialized supplier, which might contain certain residue oxygen functional groups. Another possible reason could be that there is oxygen residue in the tube vacuum furnace after purging, which oxidizes copper during sintering. Thus, CuO phase can be detected in XRD patterns though in a small amount. Secondly, the XRD patterns of the Gr-Cu nanocomposites exhibit an apparent peak at 2θ degree of 26.3°, which can be indexed to the C (002). It is shown that the composites only contain graphene and copper, in which graphene is constructed by crystalline phase carbon atoms. This implies graphene sheets are kept in the composites and survived after the vacuum sintering process.

To further confirm the presence of graphene in the vacuum sintered nanocomposites, Raman spectroscopy was employed to characterize the nanocomposites and the results were compared with the bare graphene. Note this, Raman spectroscopy has been widely utilized in the structure and defect investigation of carbon materials, such as graphite, carbon nanotubes and graphene. Fig. 3b shows the Raman spectra of the vacuum sintered Gr-Cu nanocomposites, which clearly shows the peaks at 1 344, 1 581 and 2 708 cm^{-1}, corresponding to the *D* peak, *G* peak and 2*D* peak of multilayer graphene, respectively. However, the Raman spectrum of bare graphene locates its peaks at 1 325, 1 568 and 2 568 cm^{-1}, for *D* peak, *G* peak and 2*D* peak, respectively. By compar-

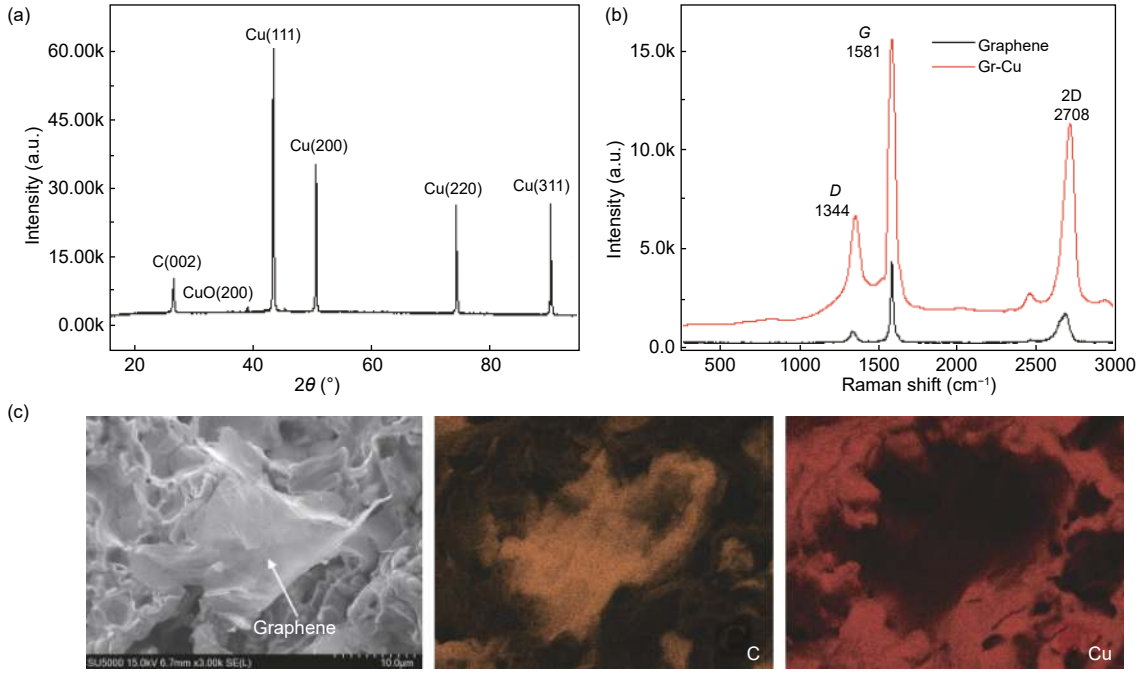

Fig. 3 (a) The XRD patterns of vacuum sintered Gr-Cu nanocomposites, (b) Raman spectra of pristine graphene and the vacuum sintered Gr-Cu nanocomposites and (c) EDS maps of carbon and copper elements in vacuum sintered Gr-Cu nanocomposite.

ing the position and intensity of those characteristic peaks, it is found that graphene peaks are downshifted and the intensity ratios of the *D* peak (I_D) to *G* peak (I_G) are also changed. This phenomenon has been mentioned in prior reports of graphene reinforced MMCs. Pavithra et al described in his paper that increment in the intensity of the I_D compared to the I_G can be observed in the Raman spectra of graphene/copper composites, and it is attributed to the stresses in graphene sheets[11]. The downshifting peaks are usually ascribed to the thermal stress induced during the sintering process. The increased intensity ratio of *D* peak to *G* peak after vacuum sintering, indicates that the structure defect level of graphene increases. Ferrari pointed out that different amounts of disorder will have different I_D/I_G in Raman spectrum[12]. Both XRD patterns and Raman spectra indeed confirm that graphene is retained in Cu matrix of the sintered nanocomposites after vacuum sintering. Although, there is a long heating time in the vacuum sintering process, graphene still manages to maintain its physical structure. This suggests long time vacuum sintering is suitable for maintaining the basic structure and properties of graphene sheets in copper matrix, and this technology can be successfully used for preparing Gr-Cu nanocomposites in other geometry or shape.

The EDS mapping is also utilized to confirm the existence of graphene sheets in Gr-Cu nanocomposites. As shown in Fig. 3c, it can be observed that one graphene sheet exists in the nanocomposite which is marked in the first SEM image. The other two images are the EDS mapping of the first SEM image, showing the map of carbon and copper elements in the cross section. Carbon EDS mapping shows the carbon element in yellow color located in the center of the cross-sectional area, with the continuous shape of graphene being observed. This confirms the completion of graphene sheets in the nanocomposite phase after vacuum sintering process. Further evidence shown in Cu EDS mapping, the copper element map clearly exhibits blank regions on the graphene position. In addition, for single layer or few layers graphene or graphene oxide, it is difficult to observe a clear-cut regime of graphene sheets or graphene oxide sheets on EDS maps of the section SEM image, provided that they are uniformly dispersed in the matrix. Our previous single layer graphene-titanium (SLGO-Ti) works verified it. On the EDS map images of SLGO-Ti, no clear-cut shape can be found[13]. Thereby, the EDS mapping shown in Fig. 3c also im-

plies a certain extent of agglomeration of graphene sheets in the nanocomposite, which requires further work to avoid this issue.

The all-aforementioned measurements including XRD, Raman and EDS confirm that graphene phase exists in the Gr-Cu composites after the vacuum sintering process. And it could be further confirmed by HRTEM images in more details. Fig. 4a is the HRTEM image of the Gr-Cu nanocomposites, which shows graphene on left side and copper on right side with their interface marked by the yellow dashed line. The inserted image in Fig. 4a is the selected area electron diffraction (SAED) pattern of graphene. In order to observe copper phase clearly, selected area of copper phase marked by the black rectangle is magnified in Fig. 4b, with corresponding SAED patterns. And also, the lattice fringes of graphene, 0.246 nm and Cu (111), 0.20 nm can be observed. The interface area between graphene and copper, as shown in the yellow dashed line surrounded area, indicates no chemical reactions with a distinct separate lattice structure. This agrees with the previous studies that no carbide phase of copper could be formed. Also, the oxide phase of copper is not observed neither. In this respect, we conclude the graphene and copper are simply overlapped and mixed together, with solely physical interaction. This suggests lower enhancement of mechanical properties achieved for copper, as compared with other reinforced metals, such as Ni, Mg and Ti with carbide phase formed serving as load transfer media. In addition, the weak bounding between graphene and copper in combination with the potential agglomeration of graphene platelets, might induce pores. Physical measurements have been conducted to assess the

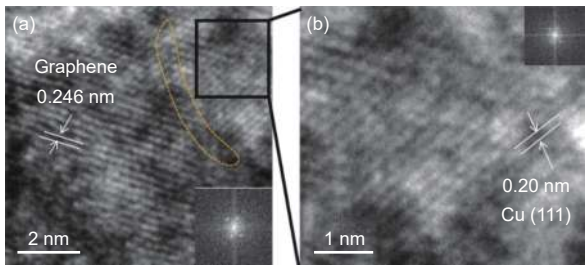

Fig. 4　HRTEM images of Gr-Cu composites: (a) graphene, Cu and their interface, with corresponding SAED patterns and (b) Cu area with the corresponding SAED pattern.

packing density to be around 70% of the theoretical one after vacuum sintering process.

In order to assess the mechanical property enhancement by graphene, samples of the pure copper, 1 wt. %, 2.5 wt. % and 5 wt. % Gr-Cu nanocomposites are made by the vacuum sintering process with a similar packing density and measured by the Vickers hardness tester. Before hardness measurement, the surfaces of all samples were polished to achieve a uniform and flatten surface, then the samples were selected randomly with each sample measured by 5 points. Fig. 5a shows the Vickers hardness values of both pure copper and nanocomposites, which are the average values of the 5 independent measurements. In Fig. 5a, the hardness values of Gr-Cu nanocomposites are plotted as a function of graphene weight ratio, within which hardness values of vacuum sintered 1 wt. %, 2.5 wt. % and 5wt. % Gr-Cu nanocomposites are 62.4, 64.4 and 51.6 HV, respectively. The highest hardness value is 45% higher as compared with the vacuum sintered pure copper (44.6 HV). It can be found that the hardness of nanocomposites would be improved with increasing the amount of graphene content. However, overdose of graphene fillers inside the nanocomposites would cause the degraded hardness value, e.g., 5wt. % Gr-Cu in Fig. 5a. This is due to the aggregation of graphene, and it is in good agreement with the surface morphology observation in Fig. 2. Previous research stated that the hardness improvement of graphene reinforced MMCs is mainly attributed to the excellent mechanical properties of graphene. Kuang et al reported significantly increased mechanical properties of graphene-nickel composites, which was attributed to the special structure and outstanding mechanical properties of homogenously dispersed graphene sheets in nickel matrix[14]. Our prior work also prepared laser sintered Gr-Cu nanocomposites[15], compared with the hardness of this study, it can be found that no matter pure copper or the Gr-Cu nanocomposites with the same graphene content, laser sintered samples have higher hardness values than the corresponding vacuum sintered ones. The reasons may be ascribed to the following three aspects. First,

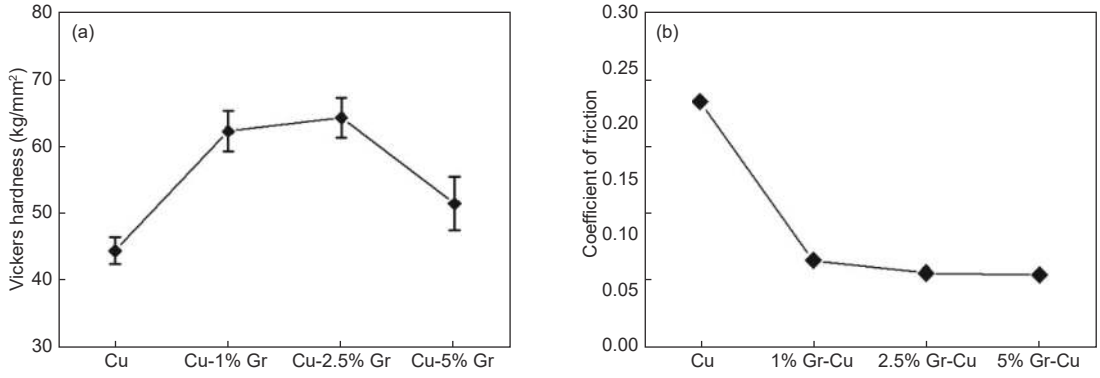

Fig. 5 (a) The Vickers hardness of vacuum sintered Cu and Gr/Cu composites and (b) effect of the graphene content on the friction coefficient of Gr/Cu composites.

laser sintering is a fast heating and cooling process, the high cooling rate will cause the composites to have fine grains and correspondingly possess a higher hardness. Meanwhile, for the vacuum sintering, the cooling rate is much lower, causing a relative lower hardness, similar to the effects of quench and annealing. Second, during laser sintering, copper powder is melted and sintered in liquid state reaction, while the highest temperature is lower than the melting point of copper in vacuum sintering. Therefore, laser sintering will yield a higher relative density. Vacuum sintering samples have several pores and relative low density, which will inevitably degrade the hardness performance. Third, less graphene agglomeration occurs during laser sintering process, in which the molten copper powder would induce a certain amount of graphene sheets floating onto the sample surface, and further lose some of graphene. Although, the accurate amount of graphene loss is not determined, it would indeed benefit the hardness performance of nanocomposites. However, unlike laser sintering process, poor performance of hardness and other mechanical properties are obtained in pressureless vacuum sintering process, since a high content of graphene will lead to agglomeration, and thereby more pores and lower relative density in the sintered composites. In this sense, the loss of graphene sheets will benefit the final mechanical performance of laser sintered graphene copper nanocomposites. Additionally, the stirring effect of laser induced melting pool further improves the dispersion homogeneity of graphene sheets in the copper matrix during laser sintering process.

The filler agglomeration degrades mechanical properties of composites is due to the 2D nature of graphene, of which the out-of-plane strength is significantly lower than the in-plane strength. Sadowski pointed out by predictions that the out-of-plane mechanical properties of graphene strongly influence the composite properties when graphene platelets are randomly oriented in the Gr-Cu composites[16]. In this respect, the agglomeration would introduce plenty of weak points, thereby lower the hardness of composites when multi-stacked graphene is applied with the mechanical force loading. This could also be confirmed by the error bars in Fig. 5a, in which pretty scattered hardness values are collected for the samples with high graphene contents.

In order to further assess the mechanical performance of the vacuum sintered nanocomposites, a sliding test with a constant sliding speed of 25 mm s^{-1} for 5 min was performed for all the designed samples. Fig. S3 shows SEM images of worn surfaces of samples, including bare copper and the Gr-Cu nanocomposites. It can be seen from these images that the nanocomposites have similar worn surface morphology, while bare Cu sample is obviously different. From Fig. S3a, it should be noticed that the worn surface of pure copper is rougher, deeper ploughing grooves can be found along the sliding direction than that of the nanocomposites containing graphene, which indicates the adhesive wear and abrasive wear behavior. All the worn surfaces of other vacuum sintered Gr-Cu nanocomposites in Figs. S3d, g and j, have a more flatness surface, and a few abrasive

grooves also can be found on these surfaces. The SEM images on the right side indicate the delamination of surface materials, which is caused by cracks and cavities, and also involved in the deformation of subsurface and development of cracks. Li et al pointed out that in the wear and friction experiments of Gr-Cu nanocomposites the nucleation of cracks in the matrix is easy to find at weak points, mainly located at the interface between graphene sheets and copper matrix, where pores have high probability to be formed. That is why crack propagation and interfacial debonding are easy to find at the copper-graphene interface, because stress concentration plays an important role during wear and friction test. This will result in delamination wear[6]. Similar phenomenon is also observed in our experiments.

A higher graphene content results in more graphene/copper interface and more agglomeration of graphene sheets, as shown in Figs. 2d and f, which would cause a higher abrasion loss. However, at the same time, more graphene sheets will expose to the contact surface, forming an isolated carbonaceous layer between the sliding ball and sample surface. The carbonaceous layer has self-lubricating property, and this can partially separate the sliding ball surface and copper matrix. So the plastic deformation can be prevented at the contact interface during the wear and friction experiments[17], and the wear rate can be minimized. As Algul et al reported in the nickel-graphene nanocomposites in their experiment results, with increasing graphene content, the tribological property of the composites become better due to the increased hardness and the fact that graphene sheets act as load bearing and solid lubrication components in the sliding surface. Meanwhile, it will have a lower and more stable friction coefficient. Fig. 5bshows the average friction coefficients of vacuum sintered copper and Gr-Cu composites with different graphene contents. It can be found that the friction coefficient of Cu is much higher than Gr-Cu nanocomposites, and it decreases from 0.22 to ~0.07 when increasing the graphene weight ratio. Although the friction coefficients of different Gr-Cu composites have a tendency to become lower with increasing graphene content, generally they have no large drop. The measured friction coefficients are lower than that of Li's report. This is mainly due to the difference of graphene content, since our process achieve much higher graphene volume contents in the Gr-Cu nanocomposites.

4 Conclusion

In this work, Gr-Cu nanocomposites were prepared by ball milling and pressureless vacuum sintering. It is confirmed by XRD, Raman and EDS that graphene flakes are well dispersed in the nanocomposites. After ball milling and vacuum sintering, graphene is mixed with copper powder homogeneously and retained in the composites after sintering. Graphene structure has no apparent physical change, but the defects in graphene flakes increase. XRD patterns, Raman spectra and HRTEM images confirm that graphene is retained in the copper matrix. This suggests the vacuum sintering process can be used to fabricate Gr-Cu nanocomposites in bulk scale. The SEM and HRTEM images and sectional EDS maps show uniform distribution of graphene sheets in the nanocomposites. The hardness of the Gr-Cu nanocomposites increases by nearly 45% and the friction properties are significantly improved as compared with the bare copper. The results indicate that graphene is an excellent strengthening material for copper and the traditional powder metallurgy method can be used to prepare the Gr-Cu nanocomposites.

Acknowledgements

Postgraduate Research & Practice Innovation Program of Jiangsu Province (KYCX17_0285), Arizona State University Startup Funding and National Science Foundation .

References

[1] Bakshi S R, Lahiri D, Agarwal A. Carbon nanotube reinforced metal matrix composites - a review[J]. International Materials Reviews, 2010, 55(1): 41-64.

[2] Neubauer E, Kitzmantel M, Hulman M, et al. Potential and challenges of metal-matrix-composites reinforced with carbon nanofibers and carbon nanotubes[J]. Composites Science and

Technology, 2010, 70(16): 2228-2236.
[3] Sun L, Fugetsu B. Mass production of graphene oxide from expanded graphite[J]. Materials Letters, 2013, 109(1): 207-210.
[4] Hu Z, Tong G, Lin D, et al. Graphene-reinforced metal matrix nanocomposites - a review[J]. Materials Science and Technology, 2016: 1-24.
[5] Bartolucci S F, Paras J, Rafiee M A, et al. Graphene-aluminum nanocomposites[J]. Materials Science and Engineering: A, 2011, 528(27): 7933-7937.
[6] Li J F, Zhang L, Xiao J K, et al. Sliding wear behavior of copper-based composites reinforced with graphene nanosheets and graphite[J]. Transactions of Nonferrous Metals Society of China, 2015, 25(10): 3354-3362.
[7] Pérez-Bustamante R, Bolaños-Morales D, Bonilla-Martínez J, Estrada-Guel I, Martínez-Sánchez R. Microstructural and hardness behavior of graphene-nanoplatelets/aluminum composites synthesized by mechanical alloying[J]. Journal of Alloys and Compounds, 2014, 615(Supplement 1): S578-S82.
[8] Kim WJ, Lee TJ, Han SH. Multi-layer graphene/copper composites: Preparation using high-ratio differential speed rolling, microstructure and mechanical properties[J]. Carbon, 2014, 69: 55-65.
[9] Chu K, Jia C. Enhanced strength in bulk graphene-copper composites[J]. Physica Status Solidi (a), 2014, 211(1): 184-90.
[10] Xu Z, Buehler M J. Interface structure and mechanics between graphene and metal substrates: A first-principles study[J]. Journal of Physics: Condensed Matter, 2010, 22(48): 485301.
[11] Pavithra L P, Sarada B V, Rajulapati K V, et al. A new electrochemical approach for the synthesis of copper-graphene nanocomposite foils with high hardness[J]. Scientific Reports, 2014, 4: 4049.
[12] Ferrari A C. Raman spectroscopy of graphene and graphite: Disorder, electron-phonon coupling, doping and nonadiabatic effects[J]. Solid State Communications, 2007, 143(1-2): 47-57.
[13] Hu Z, Tong G, Nian Q, et al. Laser sintered single layer graphene oxide reinforced titanium matrix nanocomposites[J]. Composites Part B: Engineering, 2016, 93: 352-359.
[14] Kuang D, Xu L, Liu L, et al. Graphene nickle composite[J]. Applied Surface Science, 2013, 273(0): 484-490.
[15] Zengrong H, Feng C, Dong L, et al. Laser additive manufacturing bulk graphene-copper nanocomposites[J]. Nanotechnology, 2017, 28(44): 445705.
[16] Sadowski P, Kowalczyk-Gajewska K, Stupkiewicz S. Classical estimates of the effective thermoelastic properties of copper-graphene composites[J]. Composites Part B: Engineering, 2015, 80: 278-290.
[17] Algul H, Tokur M, Ozcan S, et al. The effect of graphene content and sliding speed on the wear mechanism of nickel-graphene nanocomposites[J]. Applied Surface Science, 2015, 359: 340-348.

常压烧结法制备石墨烯-铜纳米复合材料

胡增荣[1,2]， 代 睿[3]， 王滴泥[3]， 王晓南[2,4]， 陈 峰[5]， 范学良[1]， 陈长军[6]，
廖移量[7]， 年 琼[3,*]

（1. 苏州大学 轨道交通学院 江苏 苏州 215131；
2. 苏州大学 高性能金属材料研究院 江苏 苏州 215131；
3. 亚利桑那州立大学 机械工程系 美国 亚利桑那州 坦佩 85281；
4. 苏州大学 沙钢钢铁学院 江苏 苏州 215131；
5. 南京航空航天大学 机电工程学院 江苏 南京 210016；
6. 苏州大学 机电工程学院 江苏 苏州 215131；
7. 内华达大学 机械工程系 美国 内华达州 雷诺 89557）

摘 要： 石墨烯由于具有超高强度、刚度以及优异的热学和电学性能，被认为是金属基复合材料的理想增强相。本文采用常压烧结法制备了石墨烯增强铜基纳米复合材料。采用电镜观察以及其它相应的材料表征对其微观组织及化学成分进行了研究。这些表征结果显示了常压烧结后石墨烯在复合材料中的留存及分布情况。随后对复合材料的硬度及摩擦系数进行了测试。测试结果表明石墨烯可以显著提高复合材料的硬度，同时减小其摩擦系数。

关键词： 纳米复合材料；石墨烯；铜；常压烧结

文章编号： 1007-8827(2021)02-0420-09 **中图分类号：** TB33 **文献标识码：** A

基金项目：江苏省研究生科研与实践创新计划项目（KYCX17-0285), 美国亚利桑那州立大学和自然科学基金委项目.
通讯作者：年 琼, 教授. E-mail: Qiong.Nian@asu.edu
作者简介：胡增荣. E-mail: zengronghu@126.com
本文的电子版全文由 Elsevier 出版社在 ScienceDirect 上出版（http://www.sciencedirect.com/science/journal/18725805）